DENTAL MATERIALS 26 (2010) 710–718

available at www.sciencedirect.com

ScienceDirect

journal homepage: www.intl.elsevierhealth.com/journals/dema

Effect of curing protocol on the polymerization of dual-cured resin cements

Sónia G. Pereira[a], *Rogério Fulgêncio*[b], *Teresa G. Nunes*[a,*], *Manuel Toledano*[c], *Raquel Osorio*[c], *Ricardo Marins Carvalho*[d,e]

[a] *Centro de Química Estrutural, IST (Instituto Superior Técnico), Av. Rovisco Pais, 1, 1049-001 Lisboa, Portugal*
[b] *Department of Restorative Dentistry, Universidade Federal Fluminense, Nova Friburgo, Brazil*
[c] *Department of Dental Materials, University of Granada, Granada, Spain*
[d] *Department of Operative Dentistry, University of Florida, College of Dentistry, Gainesville, FL, USA*
[e] *Department of Prosthodontics, University of São Paulo, Bauru College of Dentistry, Bauru, SP, Brazil*

ARTICLE INFO

Article history:
Received 17 August 2009
Received in revised form
15 December 2009
Accepted 9 March 2010

Keywords:
Resin cement
Dual-cured
STRAFI
Cure protocol
Extent of polymerization

ABSTRACT

Objectives. The purpose of this study was to evaluate how curing protocol affects the extent of polymerization of dual-cured resin cements.
Methods. Four commercial resin cements were used (DuoLink, Panavia F 2.0, Variolink II and Enforce). The extent of polymerization of the resin cements cured under different conditions was measured using a ^{1}H Stray-Field MRI method, which also enabled to probe molecular mobility in the kHz frequency range.
Results. Resin cements show well distinct behaviours concerning chemical cure. Immediate photo-activation appears to be the best choice for higher filler loaded resin cements (Panavia F 2.0 and Variolink). A photo-activation delay (5 min) did not induce any significant difference in the extent of polymerization of all cements.
Significance. The extent of polymerization of dual-cured resin cements considerably changed among products under various curing protocols. Clinicians should optimize the materials choice taking into account the curing characteristics of the cements.

1. Introduction

Dual-cured resin cements have been considered the material of choice to cement aesthetic indirect restorations [1]. They can be photo-polymerized or a redox initiator system can initiate the polymerization [2–5]. It is important for dual-cured resin cements to be formulated in such a way that they are capable of achieving a sufficient degree of cure with or without light-curing [2,4,6]. This is desirable to ensure adequate polymerization of the cement in areas that are not readily accessible to light. Hence, their curing kinetics involves two distinct mechanisms. They present a physical curing, induced by means of a light source, and a chemical curing, conducive to its complete curing even in the deepest recesses where the light cannot reach [6,7]. Despite their independent onset, the two ways of curing initiate a dynamics of free radical formation and monomer conversion which naturally overlap each other during the curing period. In general, the chemical-polymerizing mechanism for dual-cured resin-based materials alone is not only slower, but also less effective than when using light activation as a supplement to the final total conversion [2,8]. Recently, the influence of curing protocol on the polymerization shrinkage kinetics of dual-cured

* *Corresponding author*. Tel.: +351 21 8419043; fax: +351 21 8464455.
E-mail address: Teresa.Nunes@ist.utl.pt (T.G. Nunes).
0109-5641/$ – see front matter © 2010 Academy of Dental Materials. Published by Elsevier Ltd. All rights reserved.
doi:10.1016/j.dental.2010.03.016

resin cements (RelyX ARC, Bistite II, DuoLink, Panavia F, Variolink II and Choice) was evaluated and remarkable differences were reported on the light cure and chemical cure rates; light cure can occur about 320 times faster than chemical cure [3].

Dual-cured cement formulation includes base and catalyst pastes. As a general rule, it is known that these pastes must be mixed, applied and then photo-activated, and it can be expected that delaying or omitting the irradiation period may modify the polymeric structure [6,9,10] and the extent of polymerization (EP). While the immediate photo-activation guarantees the initial stability necessary to withstand clinical tensions, the chemical curing will guarantee the scope of its maximum properties through time and where light cannot reach. Recent evidences [6] suggest that the immediate photo-activation of some resin-based materials may compromise the final degree of conversion. Thus, the moment of light activation determines the way in which the structure networks will be formed and, as a consequence, determines the structural integrity of the materials. Insight into the effect of the moment of light activation on structural coherence, in particular in the early stages of hardening, may be of use in the clinical situation [9]. It is expected that for a given resin cement, different curing protocols may result in different degrees of cure and polymeric network cross-link density [11–13]. Resin cements that undergo different degrees of cure may present alterations in its mechanical properties [14–16]. Therefore, the characteristics of handling such as work and setting times, if changed, may influence the clinical behavior of indirect restorations cemented and their mechanical properties [7,17,20].

Usually, the degree of conversion is determined from Fourier transform infrared spectroscopy (FTIR) or calorimetric measurements. However, it has been already shown that the method of evaluation with Stray-Field Magnetic Resonance Imaging (STRAFI-MRI) is an efficient tool to produce direct evidence of the molecular mobility [18], particularly in the kHz frequency range that is increasingly restricted as monomer transforms to polymer [19]. Moreover, it is well known that mechanical properties depend strongly on molecular mobility in that frequency range, also the frequency of most of secondary mechanical relaxations. STRAFI-MRI already enabled mapping molecules from monomers until the formation of rigid polymers [20] in order to determine the extent of polymerization of resinous components [19–21]. Hence, it may be expected that, using STRAFI-MRI, a more complete evaluation of resin cements can be performed, which is based on molecular mobility analysis and is not confined to degree of conversion measurements, like FTIR. A key feature of the technique is the analysis of samples showing non-uniform polymerization. This effect is difficult or impossible to spatially resolve by FTIR or calorimetry due to experimental constraints, but can be directly evaluated by STRAFI-MRI. For instance, self- and light-curing kinetics can be better distinguished and separately analyzed using STRAFI-MRI [22]. Therefore, the aim of this study was to probe molecular mobility and EP as a function of the curing protocol of some commercially available resin cements using ^{1}H STRAFI MRI. It is hypothesized that molecular mobility and EP will vary as a function of the curing protocol and will be material dependent.

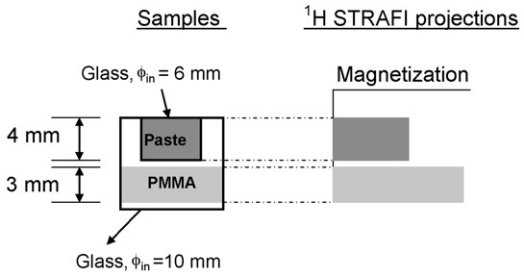

Fig. 1 – Dimensions of the PMMA reference disc and cylindrical glass containers for the ^{1}H STRAFI observation of pastes and resin cements; 1D projections (profiles) along the symmetry axes of the containers are also shown.

2. Materials and methods

2.1. *Materials*

Four dual-cured resin-based cements were examined: Enforce, DuoLink, Panavia F 2.0 and Variolink II. Table 1 shows the manufacturer, main components and the mode of application of these dental materials. They were handled in accordance to manufacturers' recommendations or using the experimental curing regimens (Table 2). Photo-activation was performed (40 s@500 mW/cm^2) using a conventional QTH light-curing unit (Optilux 401, Demetron Research Corp., Danbury, CT, USA) according to the protocols described in Table 2. All specimens were irradiated in the presence of atmospheric oxygen and the light-emission tip was always placed close to the surface. The photo-polymerization was carried out at room temperature (about 22 °C). Specimens, stored 24 h at 37 °C, in the dark, were required for the post-cured evaluation. Three samples of resin cement were prepared for every curing protocol evaluation.

2.2. *^{1}H Stray-Field MRI to probe molecular mobility and to obtain EP*

The samples (base, catalyst or mixed paste components) were placed on glass vials (6 mm internal diameter and 4 mm internal height). These vials were inserted in a cylindrical glass container (10 mm height and 10 mm inner diameter) with a 3 mm height disc made of commercial PMMA at the bottom to be used as a reference for the magnetization intensity (Fig. 1).

Each cement was prepared by mixing the appropriate amounts of the two paste components and its cure was followed-up by STRAFI according to the protocols shown in Table 2, as previously described [22]. One-dimensional ^{1}H STRAFI images, projections along an axis, were acquired from liquid pastes and cured cements, as indicated on Table 2, using a Bruker MSL 300P spectrometer, under the static magnetic field gradient of 37.5 T/m generated near the edges of the 89 mm superconducting coil. A dedicated Bruker STRAFI probe-head was tuned to 123.4 MHz, which gives ^{1}H resonance at 2.9 T; this field strength was obtained just outside the bore of the magnet. The linear resolution was about 50 μm.

Table 1 – Manufacturers, main components and mode of application of the dual-cured resin cements.

Resin cement	Main components	Mode of application
DuoLink (Bisco Inc., USA), batch nos.: A-0600010325, B-0600010326	Paste base: bis-GMA;TEGDMA;UDMA glass filler (filler content: 61.9 ± 0.43 wt%)[a]	Base and catalyst (1:1) automix from the mixing tip and light cure for 40 s according to protocols (Table 2)
	Paste catalyst: bis-GMA; TEGDMA; glass filler	
Panavia F 2.0 (Kuraray Med Company Japan), batch nos.: 00162A, 0023B	Paste A: silanated silica filler; silanated colloidal silica; MDP; hydrophilic aliphatic D; hydrophobic aliphatic D; dl-camphorquinone; catalysts; initiators	Mix paste A + B (1:1) for 20 s. Cure using: (1) Light cure each section of the cement margin for 20 s
	Paste B: silanated Ba glass; sodium fluoride; hydrophilic aromatic D; hydrophobic aliphatic D; catalysts; accelerators; pigments (filler content = 76.9 ± 0.23 wt%)[a]	or
		(2) Use Oxyguard II to cure the mixed paste. After 3 min remove Oxyguard II
Variolink II (Ivoclar Vivadent, Liechtenstein), batch nos.: K36993, K18932	Monomer matrix: Bis-GMA, UDMA and TEGDMA	
	Inorganic fillers: Ba glass, Yb trifluoride, Ba–Al–fluorosilicate glass, and spheroid mixed oxide	Mix paste A + B (1:1) for 10 s. Light cure for at least 40 s per segment.
	Additional contents: catalysts, stabilizers, and pigments (filler content = 71.2 ± 0.16 wt%)[a]	
Enforce (Dentsply, Ind e Com. Ltda, Brazil), batch nos.: 036031A, 836924B	Bis-GMA,TEGDMA, BDMA, Ti dioxide, glass fillers (filler content = 66.0 wt%)[b]	Mix paste A + B (1:1) for 20–30 s. Wait 6 min. Light cure marginal areas for 20 s from each direction

Abbreviations: Bis-GMA = 2,2 bis [4-(2-hydroxy-3-methacryloyloxypropoxy)-phenyl] propane; TEGDMA = triethylene glycol dimethacrylate; UDMA = urethane dimethacrylate; BDMA = butanediol dimethacrylate; D = dimethacrylate.
[a] Ref. [3].
[b] Ref. [4].

2.2.1. *Molecular mobility in the kHz frequency range*

^{1}H magnetization was recorded as multiple 8 spin-echo trains with echo time (TE) 35 μs and $t_{90°}$ 10 μs [21–24]. Each echo train decay, which is the magnetization decay of one sample slice, is mainly governed by the spin–spin relaxation time (T_2) that probes molecular mobility in the kHz frequency range. Data were acquired at the probe-head temperature (~22 °C). Mono-exponential functions, $M = A_1 \exp[-(x)/t_1]$, were used to fit the experimental data (trains of 8 echoes) obtained from more than two consecutive middle slices of each sample; M is the ^{1}H spin-echo magnetization recorded at the end of the echo time x, t_1 is the time-constant for the echo train decay and A_1 is a pre-exponential factor.

2.2.2. *Extension of polymerization*

1D projections (profiles) of the different samples were reconstructed using the 8 spin-echo trains acquired from each slice. Therefore, each data slice in the profiles was obtained as the summation of all the 8 echoes, which is then represented by a data point in the profiles. The magnetization of middle slices of the specimens was added up prior (slices MM) and subsequent to chemical cure, immediate or delayed light exposure (slices MPn), as indicated in Table 2. EP was obtained (in %), as follows:

$$\mathrm{EP} = \left[\frac{\sum(\mathrm{MM} - \mathrm{MPn}) \times 100}{\sum(\mathrm{MM})}\right] \quad (1)$$

The normalization of MM and MPn was based on the assignment of 1 arbitrary unit to the highest magnetization intensity obtained from the reference signal (a PMMA disc, as represented in Fig. 1). This method is based on the reasonable assumption that protons in unreacted methacrylate groups and monomers are considered to be the dominant con-

Table 2 – Description of the protocols followed to obtain the dual-cured cements and indication of ^{1}H STRAFI MRI profiles (x) recorded under each curing protocol.

Curing protocol	Description	^{1}H STRAFI profiles
I	(a) Base/catalyst mixing	x
	(b) Specimens were stored at 37 °C for 24 h, in the dark	x
II	(a) Base/catalyst mixing	–
	(b) Immediate photo-activation (40 s@500 mW/cm^2)	x
	(c) Specimens were stored at 37 °C for 24 h, in the dark	x
III	(a) Base/catalyst mixing	–
	(b) 5 min delayed photo-activation (40 s@500 mW/cm^2)	x
	(c) Specimens were stored at 37 °C for 24 h, in the dark	x

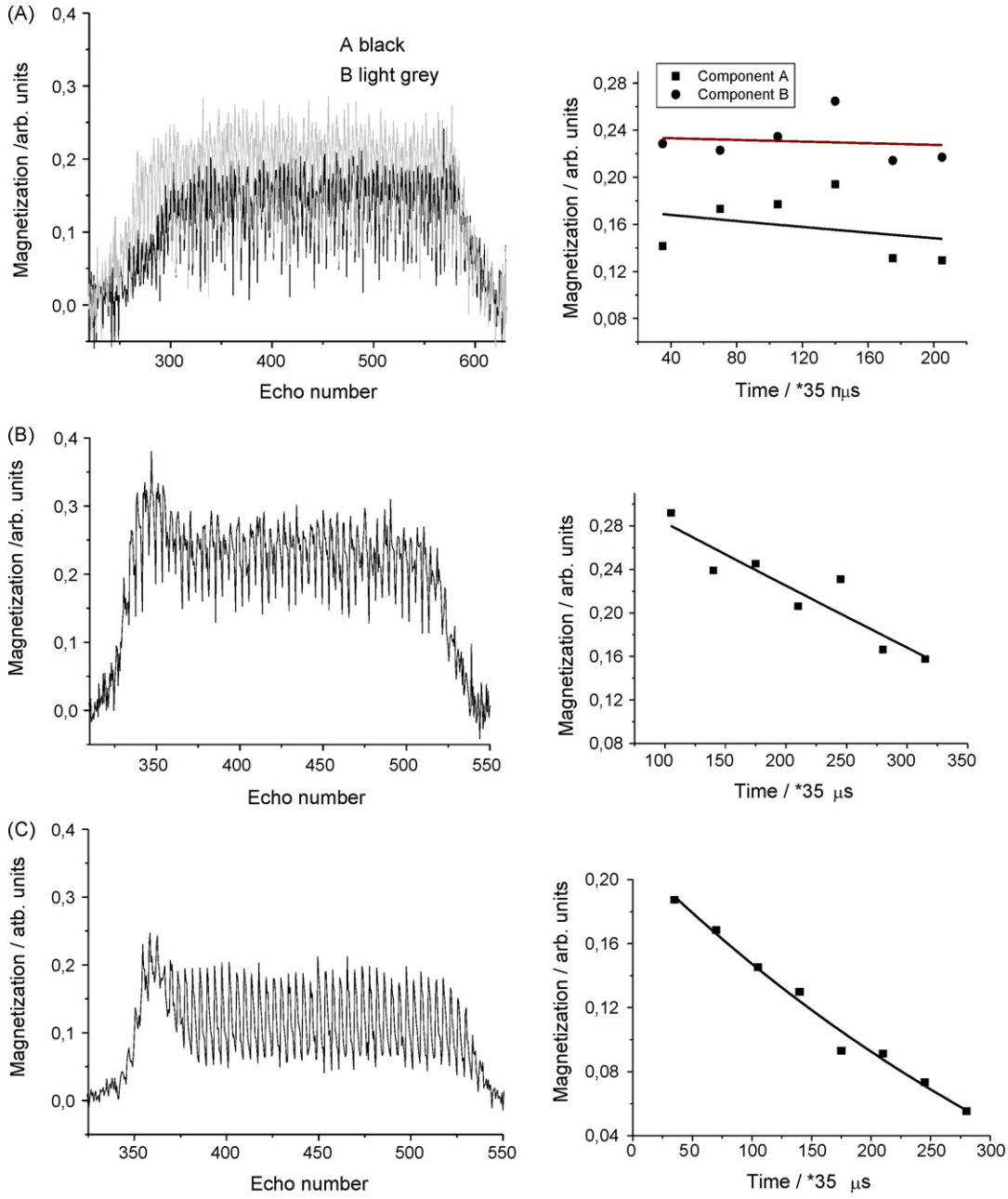

Fig. 2 – ^{1}H spin-echo magnetization obtained from PANAVIA F 2.0 base and catalyst: (A) unmixed, (B) base and catalyst mixture, (C) mixture kept 24 h at 37 °C (in the dark). The trains of echoes recorded from the middle slices of A–C are shown and the curves representing the exponential functions used to fit these experimental data are also displayed, which have the time-constants: (A) ~ 5600 μs, (B) ~ 800 μs and (C) 285 ± 40 μs.

tribution for the profiles obtained from the cured samples. Moreover, the magnetization is assumed here to be proportional to the summation of free monomer concentration and pendant unreacted methacrylate group concentration.

2.3. *Statistics*

Means and standard error of means were calculated. One-way ANOVA was used to evaluate statistical differences at a level of significance of $\alpha = 0.05$.

3. Results

Fig. 2 shows typical full ^{1}H echo magnetization decays obtained from Panavia F 2.0, which were recorded either from unmixed pastes (base and catalyst) or according to the curing protocol I. It must be noticed that, in these and subsequent figures, both the total echo magnetization decays and the corresponding profiles are rotated of 90° and, consequently, the sample surfaces are shown on the left side of the plots.

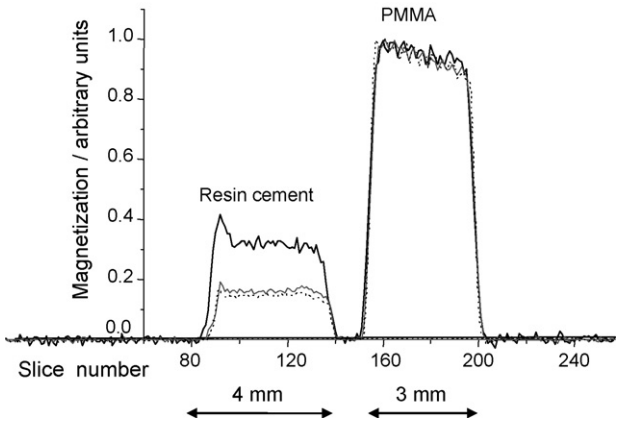

Fig. 3 – ^{1}H magnetization profiles obtained from PANAVIA F 2.0 after: (a) base and catalyst mixing (large line), (b) 40 s irradiation time (narrow line), (c) 24 h post-cure at 37 °C (dashed line).

Typical echo magnetization decays acquired from middle slices of Panavia F 2.0 samples and the curves representing the exponential functions used to fit these data are also presented in Fig. 2 (see Section 2.2.1); these functions have time-constants (t_1) ~5600 μs, ~800 μs and 285 ± 40 μs. Table 3 shows all the t_1 values obtained using exponential functions to fit the data recorded from the different resin cements under various curing conditions. Overall, higher t_1 values are expected for more mobile, hence less cured resin cements. Increasingly higher t_1 values were obtained for Enforce at the end of post-curing periods by changing the protocols from I to III (117 ± 16, 161 ± 27, 315 ± 97 μs for protocols I, II and III, respectively). Accordingly, this product shows a tendency to become more rigid when cured only chemically; a similar behaviour was obtained for DuoLink. It must be pointed out here that t_1 was also obtained for the PMMA disc used as a reference for the magnetization intensity: 221 ± 40 μs. It is possible to compare PMMA and resin cements molecular mobility in the kHz frequency range using this value and Table 3 data.

In order to obtain EP, magnetization profiles were constructed from the dual-cured resin cements, using the ^{1}H echo decays acquired according to the three protocols, as described in Section 2.2. As an illustration, Fig. 3 shows typical ^{1}H magnetization profiles obtained from Panavia F 2.0 after each curing step, according to protocol I: (a) base and catalyst mixture, (b) after 40 s photo-activation, (c) after 24 h post-cure at 37 °C, in the dark.

The first general observations are the decrease in signal intensity and the narrowing of the profiles following the reaction onset. The latter effect is clearly associated with contractions during polymerization and hence overall volume reduction. Because cured systems exhibit extensively lower magnetization, an estimate of EP, which must not be considered here as the degree of double bond conversion, could be directly drawn from magnetization measurements. The decrease of magnetization intensity with curing time is clearly associated to the loss of hydrogen mobility with evolving polymerization, in spite of the fact that the hydrogen density of

Table 3 – Magnetization integral (MI, slices 100–120, in arbitrary units) obtained for uncured pastes, for the cements after the first step of the different curing protocols and after 24 h post-cure at 37 °C, in the dark. Data obtained from uncured pastes which were used to obtain EP after the first curing step (Table 2) are underlined. Time-constants obtained for the echo train decays recorded from middle slices are shown between parentheses (t_1, μs); they were obtained by fitting exponential functions to the experimental data.

Dual-cured cement	Pastes[a]		Protocol I		Protocol II		Protocol III	
	A	B	10 min after paste mixing	Post-cure	Immediate photo-activation	Post-cure	5 min delayed photo-activation	Post-cure
ENFORCE	<u>3.08</u>	2.76	1.81 ± 0.02 (296 ± 150)	1.72 ± 0.04 (117 ± 16)	1.66 ± 0.05 (213 ± 40)	1.65 ± 0.03 (161 ± 27)	1.66 ± 0.01 (196 ± 51)	1.68 ± 0.02 (315 ± 97)
DUOLINK	<u>3.24</u>	3.05	1.82 ± 0.07 (156 ± 36)	1.66 ± 0.03 (146 ± 22)	1.60 ± 0.02 (167 ± 47)	1.61 ± 0.02 (164 ± 14)	1.61 ± 0.02 (209 ± 62)	1.62 ± 0.02 (162 ± 27)
PANAVIA F 2.0	1.94	<u>2.77</u>	3.12 ± 0.10 (~800)	1.53 ± 0.02 (285 ± 40)	1.63 ± 0.05 (–)[b]	1.49 ± 0.03 (–)[b]	1.61 ± 0.01 (–)[b]	1.45 ± 0.01 (–)[b]
VARIOLINK II	1.51	<u>1.54</u>	2.17 ± 0.10 (–)[b]	1.53 ± 0.04 (145 ± 22)	1.42 ± 0.03 (238 ± 53)	1.39 ± 0.02 (241 ± 45)	1.39 ± 0.05 (223 ± 53)	1.39 ± 0.06 (174 ± 44)

[a] Long echo trains are expected from liquids because t_1 is very long [21]; as an indication, for both Panavia F 2.0 A and B components, t_1 was about 5 ms.
[b] Large uncertainty.

each slice increases proportionally to the volume shrinkage, since the number of hydrogen atoms remains constant during the curing reaction. Hence, the observed variations could be used to determine EP throughout the reaction.

The magnetization of middle slices of the specimens was added up prior and subsequent to chemical cure, immediate or delayed light exposure, as indicated in Table 2. Table 3 shows the magnetization integrals obtained from slices 100–120 (as shown in Fig. 3 from a total of 256), positioned in the middle of the STRAFI profiles. The initial magnetization of each mixture was not determined because it is not possible, in the STRAFI MRI time scale, to detect the onset of the chemical polymerization, which starts immediately after mixing the two components; hence, base and catalyst pastes were analyzed separately in order to get approximate values of the initial magnetizations. These data must be considered as an estimation of hydrogen concentration weighted by molecular mobility of the unreacted mixed pastes, taking into account that the paste components are miscible. EP was obtained using equation 1 (see Section 2). MM and MPn data (in arbitrary units) may be directly obtained from Fig. 3.

The comparison of EP reached by the specimens (Table 4) enables establishing the protocol curing trends.

a) For the first curing step of protocols I–III:
   I) DuoLink > Enforce (undetected for Variolink II and Panavia F 2.0)
   II) DuoLink > Enforce > Panavia F 2.0 » Variolink II
   III) DuoLink > Enforce ≃ Panavia F 2.0 » Variolink II
b) EP post-curing data obtained following protocols I–III:
   I) Panavia F2.0 » Variolink II » DuoLink ≃ Enforce
   II) Panavia F2.0 » Variolink II » Enforce ≃ DuoLink
   III) Panavia F2.0 » Variolink II ≃ DuoLink ≃ Enforce

When comparing the trends shown above, the first observation is that EP obtained for the first curing step is inversely related with EP reached over post-curing periods. Overall, concerning the first step of any protocol, DuoLink and Enforce data are clearly consistent with higher chemical- and photo-activated reaction rates; higher EP was obtained before the post-curing period, regardless of the curing protocol. Accordingly, Panavia F2.0 and Variolink II results revealed ongoing reactions over the post-curing periods.

Regarding photo-activation, the cements comparative analysis indicated that Panavia F 2.0 exhibited similar post-cure effect (9.0 ± 0.7% and 9.5 ± 0.5% for protocols II and III, respectively) while Variolink only presented significant post-cure for protocol II (2.3 ± 0.3%); on the other hand, DuoLink and Enforce did not reveal statistically significant post-cure (Table 4). These results were confirmed when only chemical cure (protocol I) has occurred. The post-cure obtained for Panavia F 2.0 and Variolink II (51.1 ± 1.9% and 29.5 ± 3.1%, respectively) was statistically significant different when compared with the data obtained for DuoLink and Enforce (8.7 ± 3.8% and 5.5 ± 1.9%, respectively). It was not possible to obtain EP 10 min after mixing the paste components for both Panavia F 2.0 and Variolink II; tentative explanations are presented in the next section.

Table 4 also shows the results obtained for total EP (the most clinical relevant data), which can be summarized as fol-

Table 4 – Extent of polymerization (EP, %) obtained for the cements after the first step of the different curing protocols and after 24 h post-cure at 37 °C, in the dark. Total EP is also shown. Different letters were assigned to statistical different data ($p > 0.05$).

Dual-cured cement		Protocol I			Protocol II			Protocol III		
		EP			EP			EP		
		10 min after paste mixing	Post-cure	EP total	Immediate photo-activation	Post-cure	EP total	5 min delayed photo-activation	Post-cure	EP total
ENFORCE		39.5 ± 0.5	5.5 ± 1.9	45.0 ± 3.7^{A}	44.7 ± 1.7	0.9 ± 1.4	45.8 ± 0.8^{A}	44.7 ± 0.3	0.0 ± 0.6	44.7 ± 0.1^{A}
DUOLINK		43.8 ± 2.2	8.7 ± 3.8	51.8 ± 4.0^{B}	49.9 ± 0.7	0.0 ± 0.9	50.0 ± 0.4^{B}	49.8 ± 0.7	0.0 ± 0.3	49.8 ± 0.4^{B}
PANAVIA F 2.0	[a]		51.1 ± 1.9	51.1 ± 3.5^{B}	41.0 ± 1.8	9.0 ± 0.7	50.0 ± 1.3^{B}	42.1 ± 0.3	9.5 ± 0.5	51.6 ± 0.6^{B}
VARIOLINK II	[a]		29.5 ± 3.1	29.5 ± 9.7^{C}	7.6 ± 2.0	2.3 ± 0.3	9.9 ± 2.2^{D}	9.5 ± 3.2	0.1 ± 1.6	10.2 ± 11.2^{D}

[a] EP was not determined due to post-mixing magnetization increase (see Table 3 and text for details).

lows: Enforce, DuoLink and Panavia F 2.0 reached EP of about 45%, 50% and 51%, respectively, and did not show statistical significant differences on the curing regimen. Protocol I was the best for Variolink II because an EP of $29.5 \pm 3.1\%$ was achieved but either II or III protocol leads to similar EP (about 10%). In general, Variolink II reached the lowest EP.

4. Discussion

In contrast to conventional imaging, the STRAFI-MRI technique makes use of the fringe of the permanent magnetic field where a strong static magnetic field gradient is present. Due to this permanently applied gradient, no time is required for generating (switching) the field gradients necessary for imaging, and the period between excitation and data acquisition can be of the order of few microseconds (about 1000 times shorter than in conventional MRI). The signal intensity depends on hydrogen concentration, but is also strongly affected by relaxation. This fact is not a disadvantage of the technique; on the other hand, it allows increasing contrast, which is then based on different molecular dynamics, i.e. allows the observation of both solids and liquid components. The relaxation processes are mainly spin–spin and spin–lattice in the rotating frame relaxations, which are correlated with molecular mobility in the kHz range. They have time constants T_2 and $T_{1\rho}$, which are very short for rigid solids and longer for liquid components.

This study used four different commercially available dual-cured resin cements that present differences in their composition (Table 1). DuoLink contains the lowest amount of inorganic filler (61.9 wt%) compared with Enforce (66.0 wt%) [4], Variolink II (71.2 wt%) and Panavia F 2.0 (76.9 wt%) [3]. The polymerization of dimethacrylates produces densely cross-linked network [26] and, during the polymerization period, part of the methacrylate groups involved in the formation of the cross-linked matrix remains unreacted, specially in the case of high-molecular-weight monomers [27]. Explanations about this effect could be associated with the amount of fillers and the influence of the decrease of mobility of polymer radicals and as a consequence a decrease on the reactivity. Recently, an inverse relation on polymerization shrinkage and filler loading on some dual-cured resin cements has been reported [3].

A closer examination of the data showed in Table 3 reveals that in some cases (Panavia F 2.0 and Variolink II) the magnetization acquired about 10 min after mixing the two paste components has increased slightly (3.12 ± 0.10 and 2.17 ± 0.12 arbitrary units, respectively) as compared with data recorded from each paste component (about 2 and 3 arbitrary units for Panavia F 2.0; about 2 arbitrary units for each Variolink II component). This effect may be attributed to a viscosity decrease (leading to increased molecular mobility) due to sample heating, over the decrease in mobility due to the reaction at the early stages of polymerization; that resulting from the heat released during polymerization and calculated to $56\,kJ\,mol^{-1}$ per methacrylate double bond [25,28]. Another hypothesis that may explain the observed increase of magnetization is the formation of air bubbles produced during STRAFI observations, hence leading to a volumetric increase of resin cements. This effect was only observed for the higher filler loaded resins (Table 1).

The differences found in the extent of polymerization of the evaluated resin cements may be attributed either to differences in composition or to variations in catalyst system [29]. Thus, incomplete curing of resin cements may decrease the mechanical properties of the material. The curing protocol has a critical effect on the degree of conversion and is a major clinical factor influencing the final performance of resin-based dental materials [17]. Overall, mechanical strength depends on double bond conversion, but cross-link density also plays an important role [26]. Accordingly, it was found that the curing regimen affects surface hardness and flexural strength of resin cements; in general, reduced flexural strength was observed when delayed photo-activation and no photo-activation were used [30,31]. While similar flexural strength was obtained for Enforce, Variolink II presented very strong light-activation dependence (either immediate or delayed) and the best performance from Panavia F2.0 was for immediate light-curing.

This study shows that dual-cured resin cements have different polymerization kinetics and that the extent of polymerization changes considerably among products under various curing protocols. The deficiency of chemical-cure component can result in higher concentration of unreacted double bonds, lower hardness, and higher solubility of cements, which can influence chemical stability in oral environment. Thus, it can be expected that different dual-cured resin cements may have different behavior concerning the onset of light activation; consequently, clinicians should be aware that the materials choice has to be optimized taking into account the curing characteristics of the cements and also that the use of a different product may imply changing the recommendable application [5,30–32].

The curing protocols used in this study had little effect for Enforce and DuoLink, since high percentage of extent of cure was achieved under every tested protocol. For Panavia F 2.0 and Variolink II, photo-activation had a dominant effect on the extent of polymerization. Low polymerization shrinkage was already reported on Panavia F by chemical cure over 30 min [3] which was obtained using a bonded disc method, hence in the absence of the oxygen radical scavenger effect [33].

Flexural strength of the same four dual-cured resin cements was measured [31] as a function of the curing protocols I–III shown in Table 2 and the following trends could be established: I) DuoLink > Enforce ⟫ Panavia ⟫ Variolink; II) DuoLink ⟫ Enforce > Variolink ≃ Panavia and III) DuoLink ⟫ Variolink ≃ Enforce ⟫ Panavia. Immediate photo-activation after mixing resulted in higher flexural strength for all cements. ^{1}H STRAFI MRI data agree well with flexural strength results obtained for DuoLink, which is the lowest filler loaded cement. Moreover, lower mobility in the kHz frequency range was detected for cements cured only chemically (Table 3) and this result agrees well with the lower flexural strength tendency reported on these cements [5,31].

Hence, it can be concluded that different dual-cured resin cements show different extent of polymerization and molecular mobility, according to the curing protocol. Thus, it suggests that resin cements should be selected according to the clinical situations. For example, Panavia F2.0 and Variolink II show that they are very light dependent to obtain the maximum

EP within a reasonable period of time. Thus, they should be avoided in those situations where the light cannot reach the curable paste mixture, as indirect metallic restorations or porcelain and indirect resin restorations that are more than 2 mm thick. On the other hand, Enforce and DuoLink could be used in those situations that demand a fast setting but light-curing is not available [3] and avoided, for example, when multiple restorations need to be fixed at once [3].

5. Conclusions

1. The dual-cured resin cements show distinct behaviours concerning the chemical cure:
   a. Panavia F 2.0 and Variolink II have a very low reaction rate and no reaction was detected (using ^{1}H STRAFI-MRI), even 10 min after mixing base and catalyst.
   b. The reaction occurs very fast for DuoLink and Enforce.
   c. The products with higher filler loading (Panavia F 2.0 and Variolink II) react slower.
2. As a consequence of 1a, the photo-activation delay (5 min) was too short to enable detecting significant differences between protocols II and III.
3. Enforce and DuoLink presented similar EP, independently of the curing protocol.
4. Immediate photo-activation appears to be the best choice for Panavia F 2.0 and Variolink II.
5. As a consequence of 1b, DuoLink and Enforce should be used when photo-activation is difficult and a high curing rate is needed.
6. Panavia F 2.0 and, in particular, Variolink II have reached lower EP than Enforce and DuoLink.

Acknowledgements

This work was supported by: CAPES (Brazil, Grant number O565-07-5), the Portuguese Foundation for Science and Technology (Project PDCT/SAU-BMA/55395/2004), MAT2008-02347/MAT, and JA P07-CTS-2568, P08-CTS-3944.

REFERENCES

[1] Zuellig-Singer R, Krejci I, Lutz ZF. Effects of cement-curing modes on dentin bonding of inlays. J Dent Res 1992;71:184–6.
[2] Tanoue N, Koishi Y, Atsuta M, Matsumura H. Properties of dual-curable luting composites polymerized with single and dual curing modes. J Oral Rehabil 2003;30:1015–21.
[3] Lee IB, An W, Chang J, Um CM. Influence of ceramic thickness and curing mode on the polymerization shrinkage kinetics of dual-cured resin cements. Dent Mater 2008;24:1141–7.
[4] Fonseca RG, Santos JG, Adabo GL. Influence of activation modes on diametral tensile strength of dual-curing resin cements. Braz Oral Res 2005;19:267–71.
[5] Alpöz AR, Ertugrul F, Cogulu D, Ak AT, Tanoglu M, Kaya E. Effects of light curing method and exposure time on mechanical properties of resin based dental materials. Eur J Dent 2008;2:37–42.
[6] Arrais CA, Rueggeberg FA, Waller JL, de Goes MF, Giannini M. Effect of curing mode on the polymerization characteristics of dual-cured resin cement systems. J Dent 2008;36:418–26.
[7] Arrais CA, Giannini M, Rueggeberg FA, Pashley DH. Effect of curing mode on microtensile bond strength to dentin of two dual-cured adhesive systems in combination with resin luting cements for indirect restorations. Oper Dent 2007;32:37–44.
[8] Blackman R, Barghi N, Duke E. Influence of ceramic thickness on the polymerization of light-cured resin cement. J Prosthet Dent 1990;63:295–300.
[9] de Gee AJ, Leloup G, Werner A, Vreven J, Davidson CL. Structural integrity of resin-modified glass ionomers as affected by the delay oromission of light activation. J Dent Res 1998;77:1658–63.
[10] Kakabura A, Eliades G, Palaghias G. Na FTIR Study on the settings mechanism of resin-modified glass ionomer restoratives. Dent Mater 1996;12:173–8.
[11] Asmussen E, Peutzfeldt A. Influence of pulse-delay curing on softening of polymer structures. J Dent Res 2001;80: 1570–3.
[12] Asmussen E, Peutzfeldt A. Two-step curing: influence on conversion and softening of a dental polymer. Dent Mat 2003;19:466–70.
[13] Asmussen E, Peutzfeldt A. Bonding of dual-curing resin cements to dentin. J Adhes Dent 2006;8:299–304.
[14] Ferracane JL. Correlation between hardness and degree of conversion during the setting reaction of unfilled dental restorative resins. Dent Mater 1985;1:11–4.
[15] Rueggberg FA, Craig RG. Correlation of parameter used to estimate monomer conversion in light-cured composite. J Dent Res 1988;67:932–7.
[16] Neves AD, Discacciati JA, Orêfice RL, Jansen WC. Correlation between degree of conversion, microhardness and inorganic content in composites. Pesqui Odontol Bras 2002;16:349–54.
[17] Lovell LG, Lu H, Elliott JE, Stansbury JW, Bowman CN. The effect of cure rate on the mechanical properties of dental resins. Dent Mater 2001;17:504–11.
[18] Hunter G, Lane DM, Scrimgeour SN, McDonald PJ, Lloyd CH. Measurement of the diffusion of liquids into dental restorative by stray-field nuclear magnetic resonance imaging (STRAFI). Dent Mater 2003;19:632–8.
[19] Lloyd CH, Scrimgeour SN, Lane DM, Hunter G, McDonald PJ. The application of magnetic resonance microimaging to the visible lightcuring of dental resins3. Stray-Field nuclear magnetic resonance imaging (STRAFI). Dent Mater 2001;17:381–7.
[20] Nunes TG, Garcia FC, Osorio R, Carvalho R, Toledano M. Polymerization efficacy of simplified adhesive systems studied by NMR and MRI techniques. Dent Mater 2006;22:963–72.
[21] Pereira SG, Nunes TG, Kalachandra S. Low viscosity dimethacrylate comonomer compositions [Bis-GMA and CH3Bis-GMA] for novel dental composites; analysis of the network by stray-field MRI, solid-state NMR and DSC & FTIR. Biomaterials 2002;23:3799–806.
[22] Pires RA, Fernandez C, Nunes TG. Structural and spatially-resolved studies on the hardening of a commercial resin-modified glass-ionomer cement. J Mater Sci Mater Med 2007;18:787–96.
[23] Nunes TG, Pires R, Perdigão J, Amorim A, Polido M. The study of a commercial dental resin by ^{1}H stray-field magnetic resonance imaging. Polymer 2001;42:8051–4.
[24] Nunes TG, Guillot G, Pereira SG, Pires R. ^{1}H stray-field long spin-echo trains and MRI: novel studies on the photopolymerization of acommercial dental resin. J Phys D Appl Phys 2002;35:1251–7.
[25] Pereira SG, Reis N, Nunes TG. Spatially resolved studies on the photopolymerization of dimethacrylate monomers. Polymer 2005;46:8034–44.
[26] Sideridou I, Tserki V, Papanastasiou G. Effect of chemical structure on degree of conversion in light-cured

dimethacrylate-based dental resins. Biomaterials 2002;23:1819–29.
[27] Chung KH, Greener EH. Correlation between degree of conversion, filler concentration and mechanical properties of posterior composite resins. J Oral Rehabil 1990;17:487–94.
[28] Jakubiak J, Sionkowska A, Linden LA, Rabek JF. J Therm Anal Calorim 2001;65:435–43.
[29] Stavridakis MM, Kakaboura AI, Krejci I. Degree of remaining C=C bonds, polymerization shrinkage and stresses of dual-cured core build-up resin composites. Oper Dent 2005;30:443–52.
[30] Fulgêncio R, Toledano M, Osorio R, Aguilera FS, Osorio E, Carvalho RM. Effect of curing modes on microhardness of dual resin cements. Pan European Federation of IADR; 2008 (Abstr. no. 0558).
[31] Fulgêncio R, Toledano M, Osorio R, Aguilera FS, Osorio E, Carvalho RM. Effect of curing modes on microhardness of dual resin cements. Pan European Federation of IADR; 2008 (Abstr. no. 0557).
[32] Tango RN, Sinhoreti MA, Correr AB, Correr-Sobrinho L, Henriques GE. Effect of light-curing method and cement activation mode on resin cement knoop hardness. J Prosthodont 2007;16:480–4.
[33] Watts DC, Cash AJ. Determination of polymerization shrinkage kinetics in visible-light cured materials: methods development. Dent Mater 1991;7:281–7.